ISSN (Print) : 0974-6846
ISSN (Online) : 0974-5645
Indian Journal of Science and Technology, *Vol 8(S9), 49–61, May 2015*
DOI: 10.17485/ijst/2015/v8iS9/68564

Numerical Analysis of Melting of Nano-Enhanced Phase Change Material (NePCM) in a Cavity with Different Positions of Two Heat Source-Sink Pairs

Nasser Mostafavinia[1*], Saman Eghvay[2] and Amir Hassanzadeh[1]

[1]Young Researchers and Elite Club, Mahabad Branch, Islamic Azad University, Mahabad, Iran; nasser.mostafavi@gmail.com, amir.info@gmail.com
[2]Department of Mechanical Engineering, College of Engineering, Urmia University, Urmia, Iran; s.eghvay@yahoo.com

Abstract

Thermal energy can be stored in the three forms of sensible heat, latent heat and thermo-chemical reactions. The latent heat, i.e. the heat that is stored during phase change process, plays an important role in melting process. In the Present work, melting of a NePCM in a square cavity with different horizontal angles with two heat source-sink pairs flush-mounted on the horizontal sidewalls is investigated numerically. Four different cases are studied: Case 1. Where the sources and sinks are separately placed on two horizontal sidewalls; Case 2. Where the sources and sinks are alternately placed on two horizontal sidewalls; Case 3. Where the sources are placed on the left sides of the sinks on the horizontal sidewalls; and Case 4 where the sources and sinks are placed on down horizontal sidewalls. It is found that Case 1 with 2% weight of Al_2O_3 nanoparticle has most liquid fraction ratio comparing to the other cases. In all the cases studied, the volumetric concentration of nanoparticles of 2% would result in the highest melting rate.

Keywords: Heat Source-Sink Pairs, Nano-Enhanced Phase Change Material, Numerical Analysis

1. Introduction

Thermal energy can be stored in the three forms of sensible heat, latent heat and thermo-chemical reactions. The latent heat, i.e. the heat that is stored during phase change process, plays an important role in melting process. The solid to liquid phase change during the melting process can store a large amount of energy provided an appropriate material is chosen. Meng et al[1] introduced a new type of PCM room and they examined its thermal performance experimentally and numerically.Many numerical and experimental studies on the melting of PCMs in different enclosures have done. Zhang et al[2] studied the melting of n-octadecane in an enclosure discretely heated at a constant rate from one side and thermally insulated from the other sides. Their results showed that natural convection had a significant effect on the shape of the solid-liquid interface. The effect became more pronounced when the Stefan number was increased. Faraji and El Qarnia[3] simulated the melting of a PCM in a vertical rectangular enclosure where three volumetric protruding heat sources mounted on one of the vertical walls. They demonstrated that the bottom heat source contributed the highest heat transfer rates. Kousksou et al[4] studied numerically the melting of a PCM in a rectangular enclosure, where the vertical walls and the top wall of the cavity were insulated and the bottom wavy wall was maintained at constant temperature. It was found that by increasing the amplitude value of the bottom wavy surface, the rate of melting increased. Low thermal conductivity is a key feature of PCMs. Many researches took the advantage of adding nanoparticles

*Author for correspondence

to these materials to enhance their thermal conductivity[5–10]. As an example, Wu et al[11] employed the Hot Disk thermal constants analyzer and infrared monitoring methods for investigating the effects of Cu nanoparticles on the thermal conductivity and the phase change heat transfer of PCMs. They concluded that by adding 2 wt% of Cu nanoparticles to paraffin, the thermal conductivity enhancement of 14.2% and 18.1% occurred in solid and liquid states, respectively. Several numerical and experimental studies have been carried out on the solidification and melting of nano-enhanced PCMs (NePCMs). Kashani et al[12] performed numerical modeling of solidification of Cu-water nanofluidas a PCM in an enclosure with vertical wavy walls at different Grashhof (Gr) numbers and considered the effects of surface waviness and nanoparticle dispersion on the solidification rate. The results showed that dispersion of nanoparticle in the PCM caused a decrease in solidification time and that the surface waviness could be considered as a controlling factor for solidification time. In addition, in all the Gr numbers tested, by increasing the waviness the total solidification time increased. Hosseinizadeh et al[13] simulated numerically the unconstrained melting of NePCM inside a spherical container using RT27 and copper particles as base material and nanoparticle, respectively. They conducted the simulations for three different Stefan numbers and volume fractions of nanoparticles. The results revealed that an increase in thermal conductivity in conjunction with a decrease in latent heat would result in higher melting rate of NePCM. Arasu and Mujumdar[14] carried out a numerical study on the melting of paraffin wax dispersed with different volume fractions of Al_2O_3 in a square enclosure heated from two different sides, i.e., from below and from one vertical side. The results indicated that due to dominated natural convection in the case of vertical wall heating, the melting rate was increased. Also they found that increasing the nanoparticle content to more than 2 wt.% would weaken the natural convection due to increase in viscosity. Sebti et al[15] conducted a comprehensive numerical study to investigate heat transfer enhancement during the melting process of a PCM in a 2D square cavity through dispersion of Cu nanoparticles. They found that the nanofluid heat transfer rate increased and the melting time decreased as the volume fraction of nanoparticles increased. Ho and Gao[16] carried out the melting experiments of n-octadecane dispersed with Al_2O_3 nanoparticles in a vertical square enclosure. The vertical side walls were differentially heated isothermally while the remaining side walls were thermally insulated. The results indicated that natural convection heat transfer into the melted region of the enclosure degraded significantly with increasing the mass fraction of nanoparticles dispersed in the NePCM as compared to that of the base PCM. Zeng et al[17] accomplished experimental investigation on melting of 1-dodeconal dispersed with various loadings of multi-walled Carbon Nanotubes (CNTs) in a bottom-heated vertical cylindrical cavity. Their investigations showed that in the presence of the CNTs, the melting rate was reduced as a result of increased viscosity, leading to significant weakness of natural convection during melting. They concluded that the competing effect between the enhanced heat conduction and weakened natural convection determines the melting rate of NePCMs. El Hasadi and Khodadadi[18] simulated numerically the effect of nanoparticles size on the solidification process of NePCM. Their results showed that by decreasing the nanoparticle size from 5nm to 2nm, solid-liquid interface was changed from a stable planar shape to an unstable dendritic structure. Dhaidan et al[19–21] investigated experimentally and numerically melting of paraffin (n-octadecane) with CuO nanoparticle suspensions in geometrically different enclosures including a square cavity, a horizontal cylindrical capsule and an annulus subjected to a constant heat flux. Their results clarified that the heat transfer augmented with increasing the loading of nanoparticles due mainly to an increase in thermal conductivity. Jourabian et al[22] investigated numerically the effects of nanoparticles volume fraction and the position of the hot cylinder in the melting process of Cu/water nanofluid PCMs in an annulus using enthalpy-based LBM. The objective of this study is to investigate numerically the effect of different horizontal angels of cavity with one heat source-sink pair located on the vertical sidewalls of a square cavity on the melting rate of paraffin wax as PCM dispersed with Al_2O_3 as nanoparticle in the cavity. The rest parts of the cavity walls are adiabatic. Three different volume fractions of nanoparticles (i.e., 0 wt.%, 2 wt.% and 5 wt.%) are examined. The dimension of the cavity is H H (25mm × 25mm).

2. Physical Model

The problem under consideration is the melting of a NePCM in a 2-D square cavity of side length

25mm × 25mm. In the first case the Horizontal walls are thermally insulated (Figure 1). The heat sources are maintained at a constant temperature of 330K above the melting point. The sinks' temperature is maintained at the constant temperature of 300K. The enclosure is completely filled with paraffin wax containing 0wt.%, 2wt.% and 5wt.% of Al_2O_3 as nanoparticles for enhancement of thermal conductivity. The initial temperature of PCM/Al_2O_3 is considered 300K. In addition, the following assumptions are made in present work:

- Paraffin wax as PCM is pure and in its liquid phase is incompressible and Newtonian.
- Viscous dissipation, thermal radiation, three-dimensional convection and volumetric expansion are negligible.
- The paraffin wax and Al_2O_3 nanoparticles are considered as continuous media, they are assumed to be in thermodynamic equilibrium and no-slip boundary condition is applied between them.
- The thermo-physical properties of the PCM and NePCM are assumed temperature dependent.
- The melting is an unsteady process and the flow is laminar and two-dimensional.

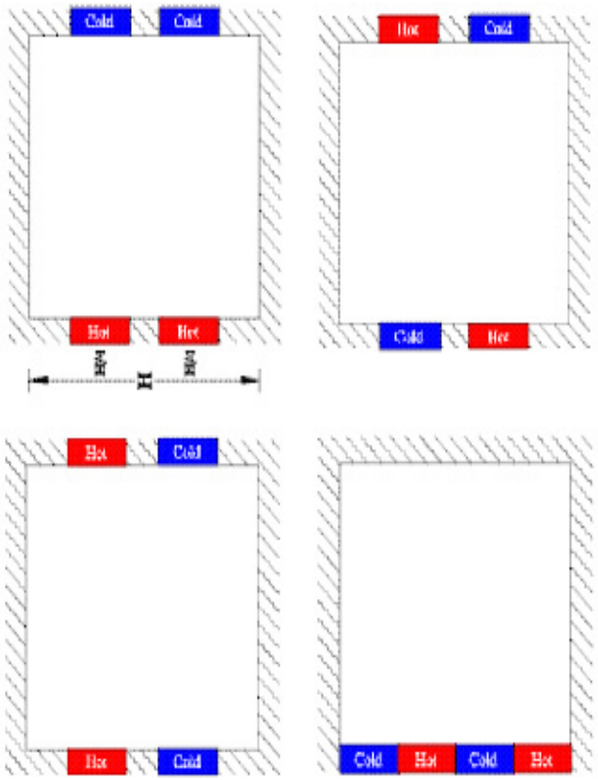

Figure 1. Six different arrangements (cases) of horizontal degree with one heat source-sink pair.

3. Mathematical Formulation and Numerical Implementation

3.1 Governing Equations

An enthalpy-porosity technique is used to simulate the melting of a NePCM in a square cavity with different horizontal degrees. Instead of tracking the solid-liquid interface explicitly, the enthalpy porosity technique computes a quantity called the liquid fraction in each cell in the computational domain at any iteration, based on enthalpy balance. In the melting process, the liquid fraction changes between 0 and 1. It possesses the values of 0 and 1 respectively for solid state and liquid state and lies between 0 and 1 for the so-called mushy state.

The continuity, momentum, and energy equations for the 2-D transient laminar flow including buoyancy-driven convection can be expressed as,

Continuity equation:

$$\frac{\partial \rho}{\partial t} + \nabla.\left(\rho \vec{V}\right) = 0 \quad \text{.....(1)}$$

In this study $\frac{\partial \rho}{\partial t}$ is zero due to incompressibility of the fluid flow after melting occurs.

Momentum equation:

$$\frac{\partial}{\partial t}\left(\rho \vec{V}\right) + \nabla.\left(\rho \vec{V}\vec{V}\right) = -\nabla P + \rho \vec{g} + \nabla.\bar{\bar{\tau}} + \vec{F}, \quad \text{.....(2)}$$

where P denotes the static pressure, $\bar{\bar{\tau}}$ is the stress tensor, $\rho \vec{g}$ and $\vec{F}$ are the gravitational and external body forces, respectively.

Energy equation:

$$\frac{\partial (\rho H)}{\partial t} + \nabla.\left(\rho \vec{V} H\right) = \nabla.(k \nabla T) + S \quad \text{.....(3)}$$

where denotes the enthalpy of the NePCM, ρ is density of the NePCM, stands for the thermal conductivity of NePCM, k is the velocity and $\vec{V}$ is the temperature. Here S is volumetric heat source term, which is set to zero in the present study.

The total enthalpy H is computed as the sum of the sensible enthalpy, h and the latent heat, ΔH,

$$H = h + \Delta H \quad \text{.....(4)}$$

Where,

$$h = h_{ref} + \int_{T_{ref}}^{T} C_p dT \quad \text{.....(5)}$$

Here, h_{ref} and T_{ref} denote the reference enthalpy and reference temperature, respectively and and C_p represents

the specific heat at constant pressure.

The latent heat in terms of the latent heat of the PCM, L is written as:

$$\Delta H = \alpha L \quad \text{.....(6)}$$

where α is the liquid fraction and is defined as:

$$\alpha = \begin{cases} 0 & ; \quad if\ T < T_{solidus} \\ \dfrac{T - T_{solidus}}{T_{liquidus} - T_{solidus}} & ; \quad if\ T_{solidus} < T < T_{liquidus} \\ 1 & ; \quad if\ T > T_{liquidus} \end{cases} \quad \text{...(7)}$$

The energy Equation (3) and the liquid fraction Equation (6) are coupled. This would necessitate iteration between them to solve for temperature. In the enthalpy-porosity technique the mushy region (partially solidified region) is considered as a porous medium. The porosity in each cell is set equal to the liquid fraction in that cell. The porosity in fully solidified regions is set equal to zero, which extinguishes the velocities in these regions.

3.2 Boundary and Initial Conditions

The heat source and sink are considered as constant-temperature boundary conditions and the rest portions of the cavity walls are made adiabatic. The initial condition is set equal to the temperature of heat sinks.

3.3 Thermo-Physical Properties

The thermo-physical properties of the pure paraffin wax and the solid nanoparticles, which were used in the present work are found in[6,7] and are also given in Table 1.

The thermo-physical properties of the NePCM are calculated from the following relations where the subscripts *np* and *pcm* stand for nanoparticles and PCM, respectively.

Density:

$$\rho_{npcm} = \varphi\rho_{np} + (1-\varphi)\rho_{pcm} \quad \text{.....(8)}$$

Specific heat capacity:

$$C_{p,npcm} = \frac{\varphi(\rho C_p)_{np} + (1-\varphi)(\rho C_p)_{pcm}}{\rho_{npcm}} \quad \text{.....(9)}$$

Latent heat[12]:

$$L_{npcm} = \frac{(1-\varphi)(\rho L)_{pcm}}{\rho_{npcm}} \quad \text{.....(10)}$$

Dynamic viscosity:

$$\mu_{npcm} = 0.983\, e^{(12.959\varphi)}\mu_{pcm} \quad \text{.....(11)}$$

The effective thermal conductivity is calculated from the following correlation proposed by Vajjha et al[9], which is a combination of Maxwell's theory (first term on the right hand side) and Brownian motion (second term on the right hand side):

Table 1. Thermo-physical properties of paraffin wax[6] and Al_2O_3[7]

Thermo-Physical Property	Al_2O_3 Nanoparticles	PCM (Paraffin Wax)
Thermal Conductivity (W/mK)	36	0.21 if $T<T_{solidus}$ 0.12 if $T>T_{liquidus}$
Solidus Temperature (K)	-	319
Liquidus Temperature (K)	-	321
Specific Heat (J/kgK)	765	2890
Latent Heat of Fusion (J/kg)	-	173400
Dynamic Viscosity (Ns/m^2)	-	0.001exp(-4.25+1790/T)
Density (kg/m^3)	3600	750/(0.001(T-319.15)+1)
Diameter of nanoparticle (m)	59×10^{-9}	-

$$k_{npcm} = \frac{k_{np} + 2k_{pcm} - 2(k_{pcm} + k_{np})\varphi}{k_{np} + 2k_{pcm} + (k_{pcm} - k_{np})\varphi} k_{pcm} + 5 \times 10^{4} \beta_k \text{ß} \varphi \rho_{pcm} C_{p,pcm} \sqrt{\frac{\kappa T}{\rho_{np} d_{np}}} f(T, \varphi) \quad \text{.....(12)}$$

Where the factor β_k for Al_2O_3 is given by:

$$\beta_k = 8.4407(100\varphi)^{-1.07304} \quad \text{.....(13)}$$

ß is the correction factor in the Brownian motion term defined as:

$$\text{ß} = \begin{cases} 0 & if\ T < T_{solidus} \\ \dfrac{T - T_{solidus}}{T_{liquidus} - T_{solidus}} & if\ T_{solidus} < T < T_{liquidus} \\ 1 & if\ T > T_{liquidus} \end{cases} \quad \text{.....(14)}$$

The Boltzmann constant κ takes the value of 1.381×10^{-23} (J/K), and $f(T, \varphi)$ is obtained from the experimental data as:

$$f(T, \varphi) = (2.8217 \times 10^{-2}\varphi + 3.917 \times 10^{-3})\frac{T}{T_0} + (-3.0669 \times 10^{-2}\varphi - 3.91123 \times 10^{-3}) \quad \text{.....(15)}$$

Where isset equal to 273K.

Figure 2 depicts the variations of the effective dynamic viscosity and thermal conductivity of paraffin wax dispersed with 0%, 2% and 5% of Al_2O_3 nanoparticles as a function of temperature obtained respectively from the Equations 11 and 12. The variations of thermal conductivity and dynamic viscosity of NePCM with volume fraction and temperature are reasonably in good agreement with the experimental results reported with Ho and Gao[14]. It is seen from Figure 2(a) that the dynamic viscosity increases with volumetric concentration of Al_2O_3 nanoparticles and decreases with temperature. However, the increase in the dynamic viscosity due to the volumetric concentration of nanoparticles is more appreciable at (relatively) low temperatures. The dynamic viscosity enhancement can affect the NePCM melting process especially when the natural convection can be assumed as the dominant heat transfer mechanism. Figure 2(b) shows that the NePCM thermal conductivity increases with the volumetric concentration of nanoparticles and decreases with the temperature.

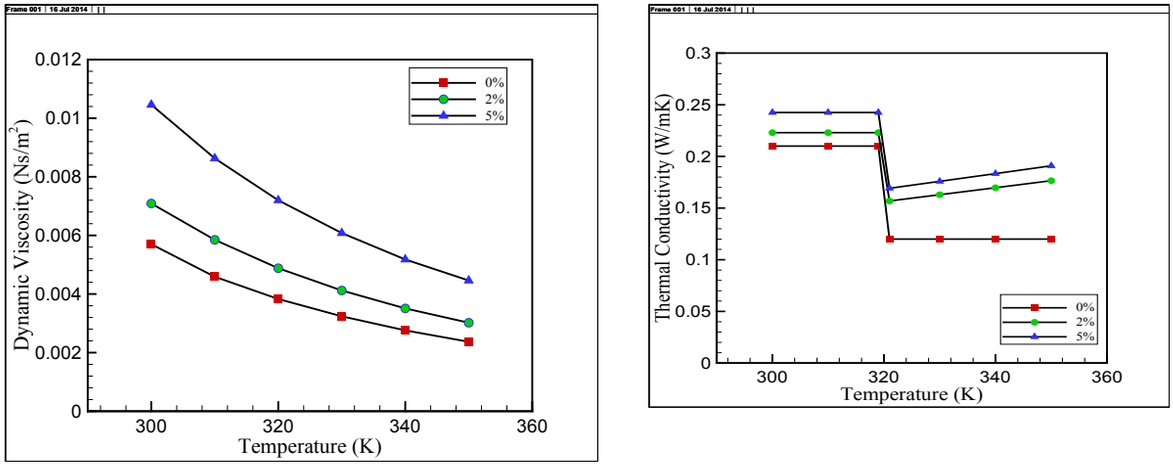

Figure 2. Variations with temperature of dynamic viscosity. (a) Thermal conductivity. (b) PCM dispersed with different volume fractions of Al_2O_3 nanoparticles.

3.4 Solution Procedure

The governing equations are solved subject to the boundary and initial conditions. These computations applied the finite volume method (using the commercial software FLUENT 6.3.26 along with GAMBIT 2.3.16). to solve the flow field equations. At the first step, a non-uniform grid is used (Figure 3). The PISO algorithm is utilized for pressure-velocity coupling whereas the PRESTO scheme is adopted for the pressure correction equation. The first order upwind scheme is used to discretize the momentum and energy equations.

In order to define the temperature-dependence of the PCM thermo-physical properties, the User-Defined Functions (UDFs) were developed. The time step for integrating the temporal derivatives was considered to be 0.001 s for the first several iterations and then was changed to 0.1 s. The number of iterations for every time step is fixed at 10 to satisfy the convergence criteria of 10^{-3} for the continuity and momentum equations, and 10^{-6} for the energy equation. The under-relaxation factors for x- and y-components of the momentum, pressure correction and energy equations are set equal to 0.5, 0.3, and 1 respectively. This value for the liquid fraction is assumed equal to 1.

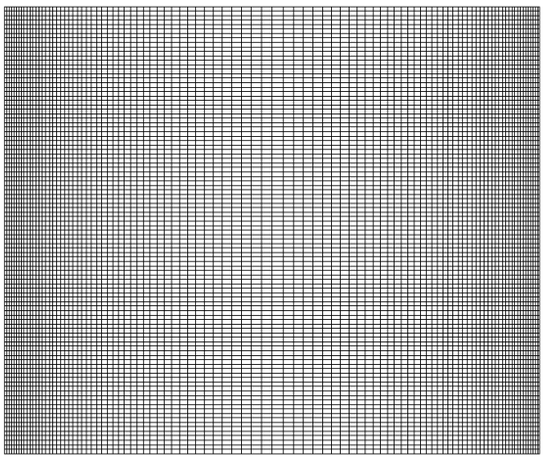

Figure 3. Typical computational non-uniform grid.

3.5 Grid Independence Test

In order to analyze the grid independence study for the obtained results, a mesh refinement was carried out (Figure 4). This procedure has been done, for liquid fraction pertaining to the Case 1 (Figure 1.) with 0 wt.% of Al_2O_3. Three different grid sizes including 80 × 80, 100 × 100 and 110 × 110 are utilized to perform the grid independence test. The relative error of liquid fraction between case 2 and case 3 is very small, and the mesh number of 100 × 100 is chosen finally considering the validity, stability and accuracy of the numerical data and the computer resource.

4. Validation of the Model

In order to substantiate the accuracy of the current numerical results, first we simulate the melting of paraffin wax as PCM dispersed with 2wt.% of Al_2O_3 nanoparticles in a square enclosure and compare the results at three different times with those reported by Arasu and Mujumdar[14]. In first validation case the vertical side hot wall is at a constant temperature of 330 K while the cold wall, facing the hot wall, is at 300 K. the bottom and top walls are kept adiabatic. And in the second case the cavity has been turned with a non-clockwise 90 degree angle. The results are depicted in terms of streamlines and isotherms (Figures 5 and 6) and liquid-solid interface (Figure 7). A reasonably good agreement is obtained.

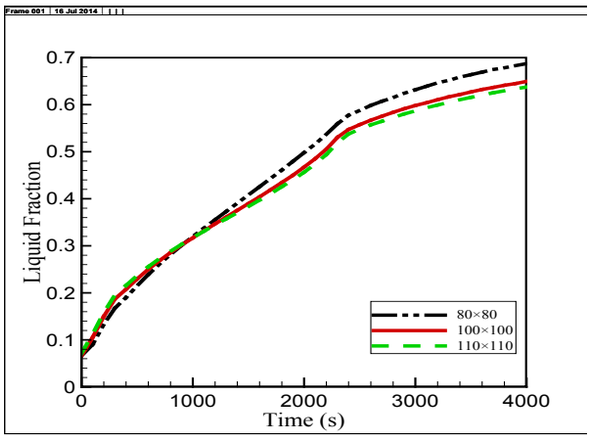

Figure 4. Effect of the grid size on the variations of the liquid fraction with time associated with the Case 1 for pure PCM.

5. Results and Discussion

As mentioned above, in the present work, the melting of paraffin wax as PCM dispersed with different volumetric concentration of Al_2O_3 nanoparticles in a square cavity with discrete heating is investigated. As shown in Figure 1, four different cases are studied: Case 1. Where the sources and sinks are separately placed on two horizontal sidewalls; Case 2. Where the sources and sinks are alternately placed on two horizontal sidewalls; Case 3. Where the sources are placed on the left sides of the sinks on the horizontal sidewalls and Case 4. Where the sources and sinks are placed on down horizontal sidewalls.

5.1 Case 1

The results associated with the Case 1 for 0 wt.%, 2 wt.% and 5 wt.% of nanoparticles are shown in Figures 8–11, respectively and are given in terms of liquid-solid interface, isotherms, velocity vectors and liquid fraction.

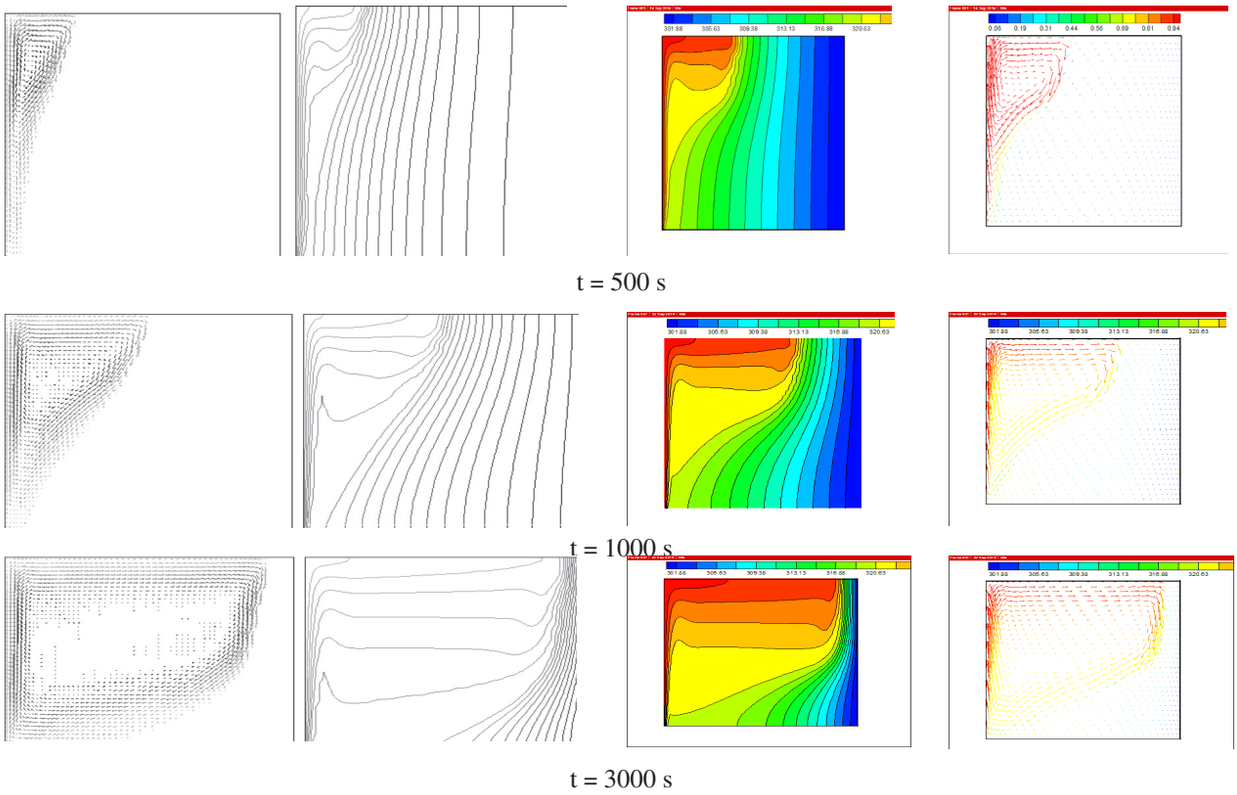

Figure 5. Comperation of present results in terms of velocity vectors and isotherms with those of 14 for parrafin wax with 2wt.% of Al_2O_3 nanoparticles in a vertical cavity.

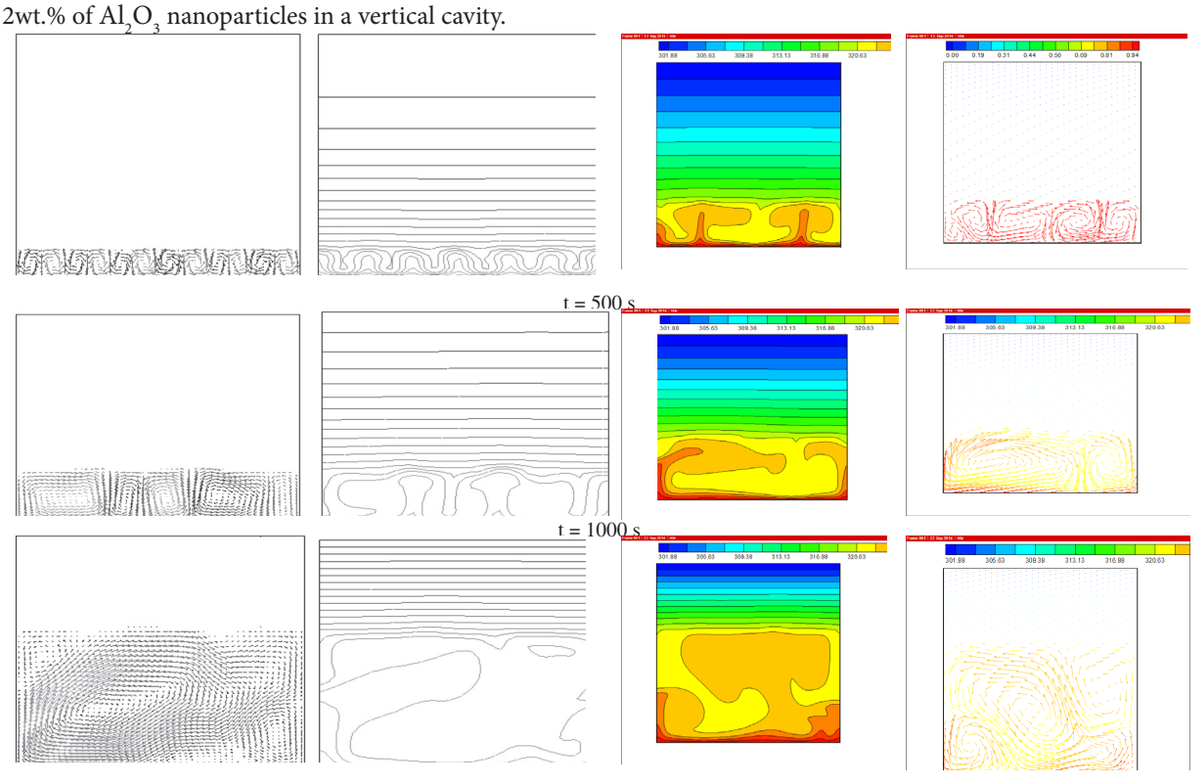

Figure 6. Comperation of present results in terms of velocity vectors and isotherms with those of 14 for parrafin wax with 2wt.% of Al_2O_3 nanoparticles in a horizontal cavity.

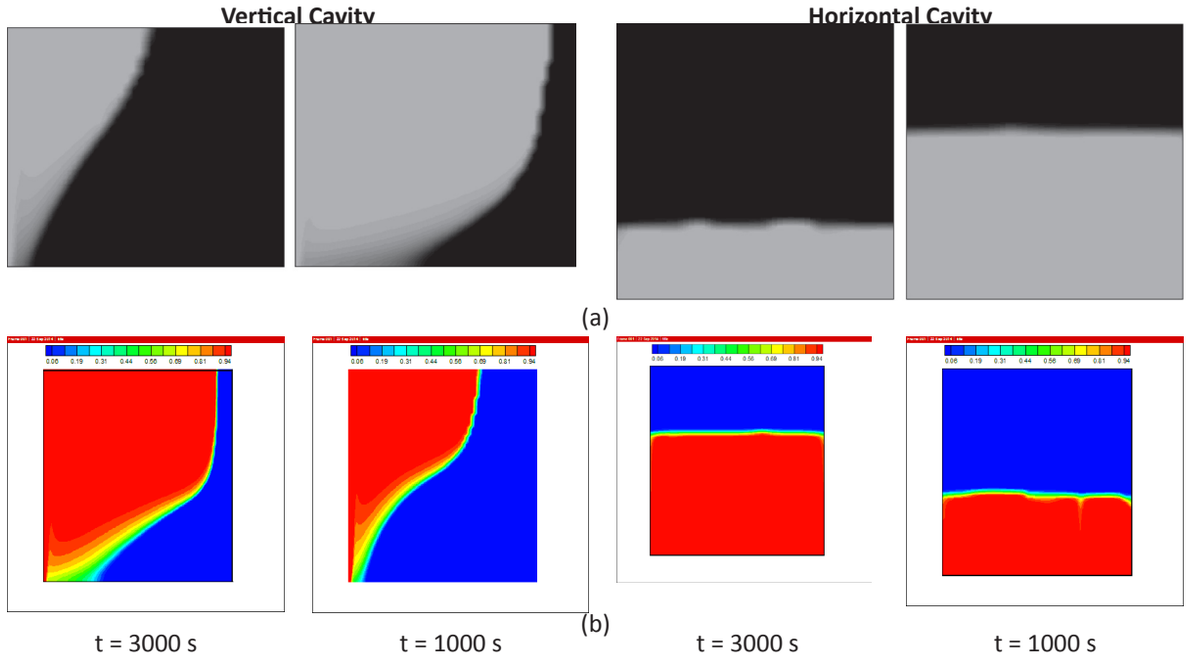

Figure 7. (a) Comparison of solid-liquid interface between Arasu and Mujumdar work[14]. (b) Present work at $t = 1000s$ and $t = 3000s$ or parrafin wax with 2wt. % of Al_2O_3 nanoparticles.

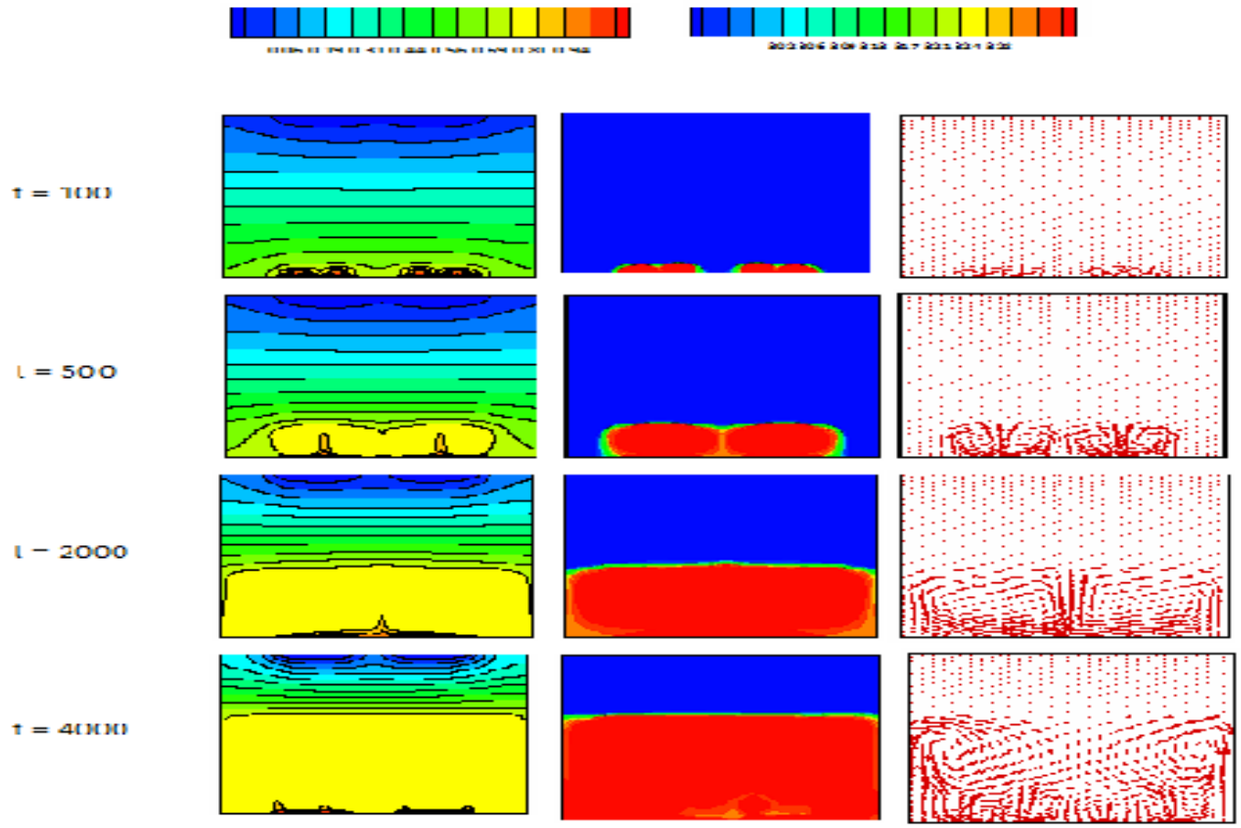

Figure 8. Liquid-solid interface (left), isotherms (middle) and velocity vectors (right) associted with the Case 1 for paraffin wax with 0wt.% of Al_2O_3 nanoparticles.

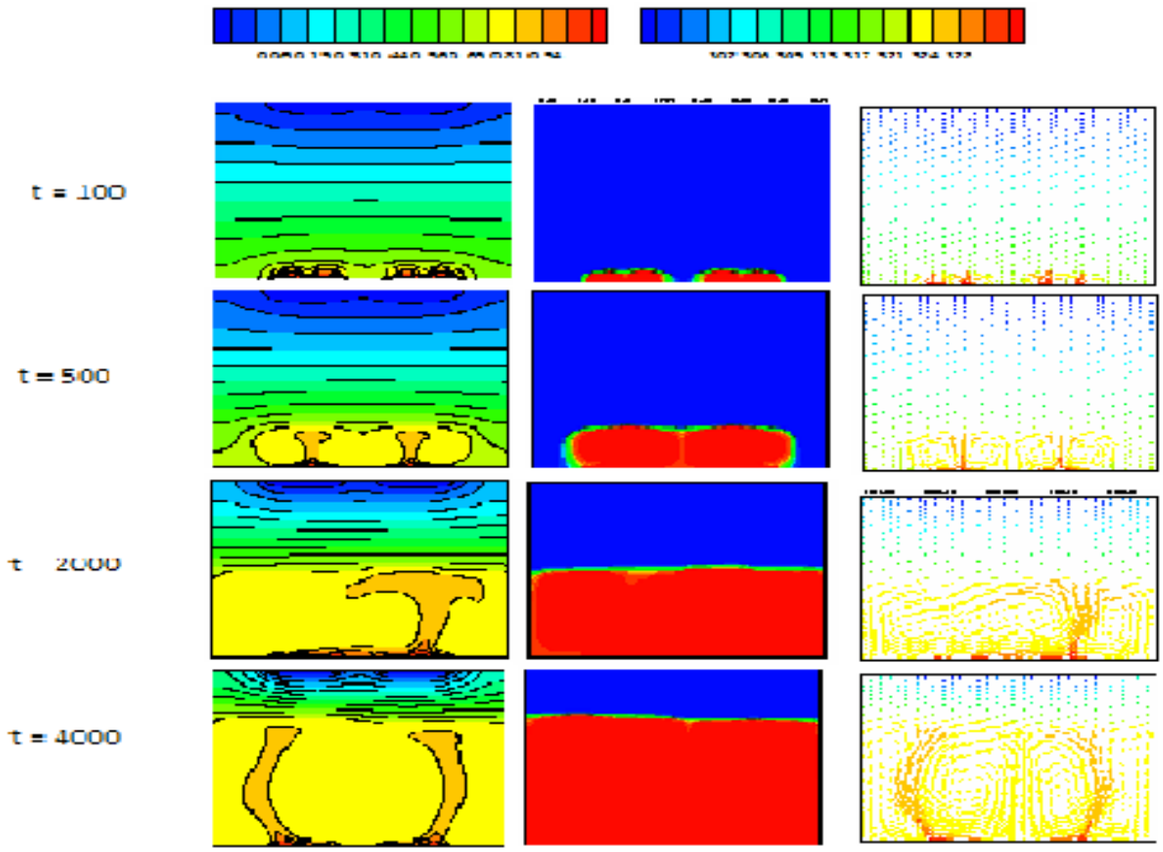

Figure 9. Liquid-solid interface (left), isotherms (middle) and velocity vectors (right) associted with the Case 1 for paraffin wax with 2wt. % of Al_2O_3 nanoparticles.

5.1.1 Liquid-Solid Interface

For all the volumetric concentrations, the liquid-solid interface, which is fairly flat at the initial stages of the melting process, becomes more and more distorted as the time passes. During the melting process, natural convection of the liquid phase is developed, which causes the hot liquid PCM near the sources to ascend and the cold liquid PCM to descend. As a result, the temperature in the upper region of the liquid becomes higher than that in the lower region, hence accelerating the melting process in the upper part. Therefore, the liquid-solid interface is more advanced near the upper region of the cavity.

5.1.2 Isotherms

For all the volumetric concentrations, it can be seen that at the initial stages of melting process (images at t = 100 s) the isothermal lines are parallel to the heat source. This would imply that the conduction is the dominated heat transfer mechanism. However, even the very small contribution of the natural convection can cause the heat to transfer toward the top part of the sources and more amount of PCM be melted there. As the time advances, the natural convection becomes the dominant mode of heat transfer, which can also be deduced from the distorted isotherm lines. This causes the heat to traverse from the sources toward the top region of the cavity, hence accelerating the melting process in this region.

5.1.3 Velocity Vectors

At the onset of melting process, the solid NePCM starts changing to liquid in close proximity to the heat sources. At the early stages of melting process, a semi-identical clockwise circulation is generated. Finally, the circulation will be more and greater as the time is advanced.

5.1.4 Liquid Fraction (A Measure of Melting Rate)

Although the liquid-solid interface images seem identical for all the three loadings of nanoparticles, however there are differences between the amounts of melted NePCM

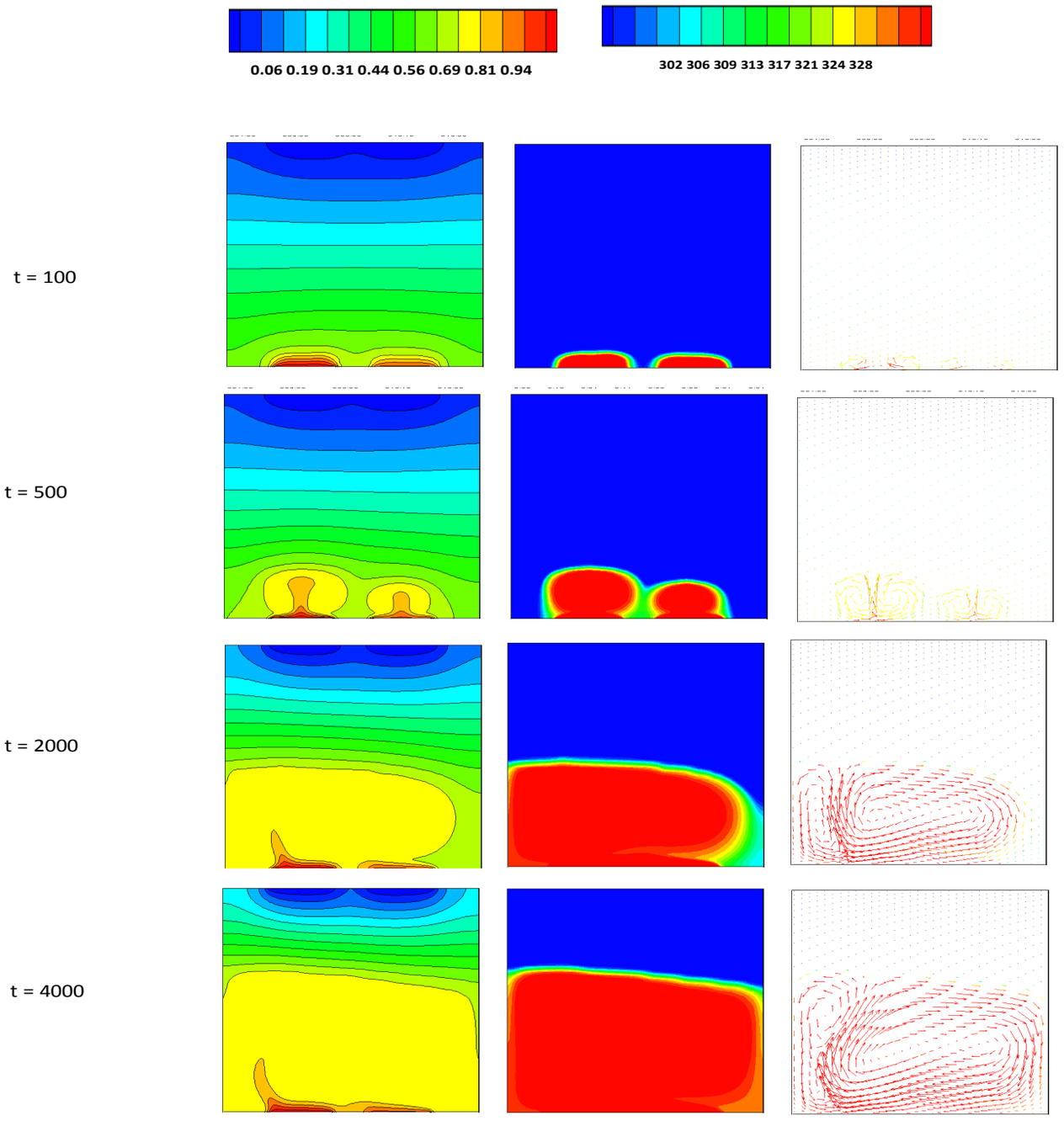

Figure 10. Liquid-solid interface (left), isotherms (middle) and velocity vectors (right) associted with the Case 1 for paraffin wax with 5wt.% of nanoparticles.

for the three loadings as shown in Figure 11. It can be seen from this figure that the rate of melting increases with the increase in volumetric concentration of nanoparticles by 2 wt. %. Also, it is seen that the melting rate of 5% Al_2O_3 is almost the same as that of the pure paraffin wax.

5.2 Cases 2-4

It was observed in the Case 1 that $\varphi = 2\%$ gave rise to the higher melting rate. This is also the case for the other three cases studied in the present work (Figure 12). As observed from Figure 12, both the dynamic viscosity and the thermal conductivity of the PCM increase with

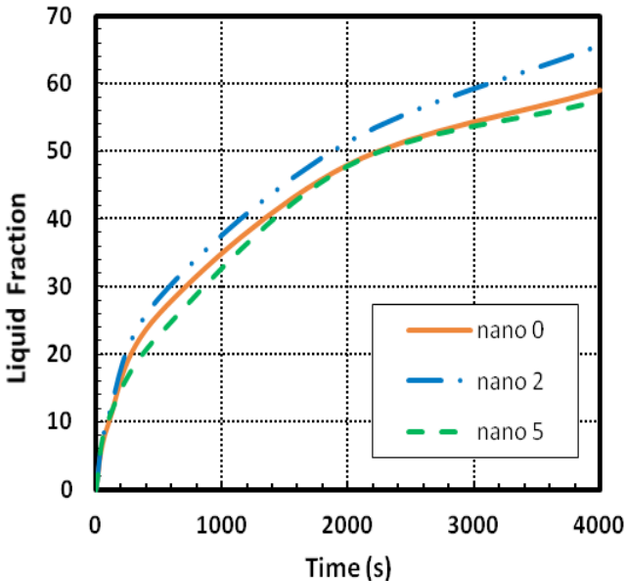

Figure 11. Variations of the liquid fraction for three different loadings of nanoparticles for Case 1.

volumetric concentration of nanoparticles and decrease with temperature. However, the increase in the dynamic viscosity with the volumetric concentration of nanoparticles is more appreciable at (relatively) low temperatures. The enhancement in the dynamic viscosity can affect the melting process of the NePCM especially when the natural convection is the dominant heat transfer mechanism. At low temperatures, the dynamics viscosity of NePCM has negative effect on the natural convection so that it can deteriorate the positive effect of increasing in conductivity. This is the reason why for $\varphi = 5\%$ the melting rate is lower than its counterpart for $\varphi = 0\%$ and 2%.

For all the volumetric concentrations, the liquid-solid interface, which is fairly flat at the initial stages of the melting process, becomes more and more distorted as the time passes. During the melting process, natural convection of the liquid phase is developed, which causes the hot liquid PCM near the sources to ascend and the cold liquid PCM to descend. As a result, the temperature in the upper region of the liquid becomes higher than that in the lower region, hence accelerating the melting process in the upper part. Therefore, the liquid-solid interface is more advanced near the upper region of the cavity. Figure 12 shows the amounts of melted NePCM for the three loadings of Al_2O_3 nanoparticles for cases II to IV. Although the liquid-solid interface images seem identical for all the three loadings, however there are differences between the amounts of melted NePCM.

It can be seen from these figures that the rate of melting increases with the increase in volumetric concentration of nanoparticles by 2 wt.%. Also, it is seen that the melting rate of 5% Al_2O_3 is almost the same as that of the pure paraffin wax.

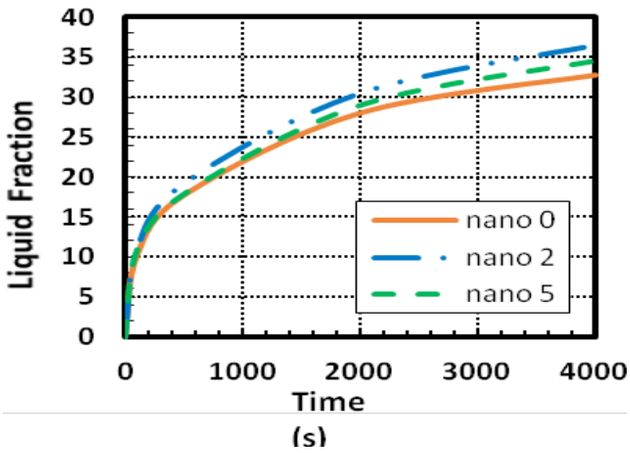

Case 2

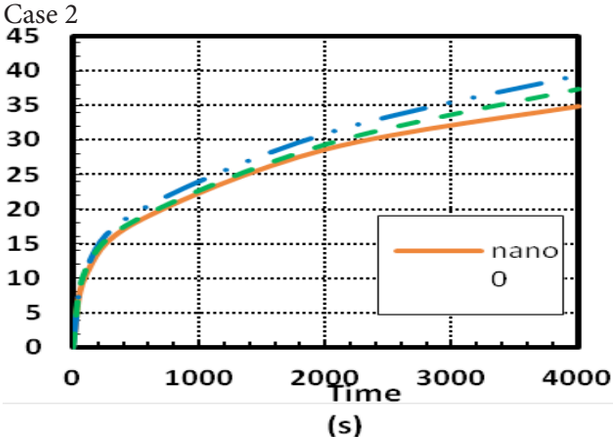

Case 3

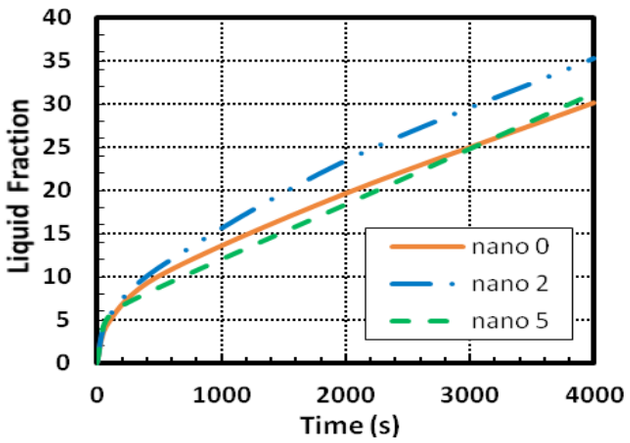

Case 4

Figure 12. Variations of the liquid fraction for three different loadings of nanoparticles for Case 2 to 4.

5.3 Effect Source-Sink Positions on the Melting Rate

Comparison between different cases studied in the present work shows that for all the volumetric concentration of Al_2O_3 nanoparticles, the Case 1 has the highest liquid fraction and the Case 4 possesses the lowest liquid fraction at $t = 4000\ s$ (Figure 13, Figure 14 and Figure 15).

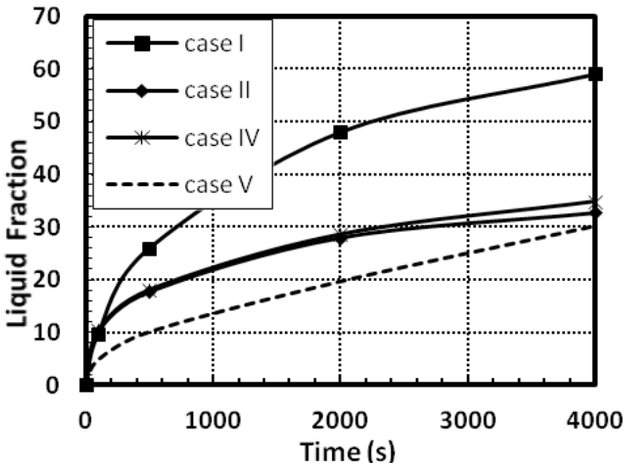

Figure 13. Left: Comparison of liquid fraction between different cases for paraffin wax with 0wt. % of Al_2O_3 Right: Liquid-solid interface at t = 4000 (s) for all cases for paraffin wax with 0wt. % of Al_2O_3.

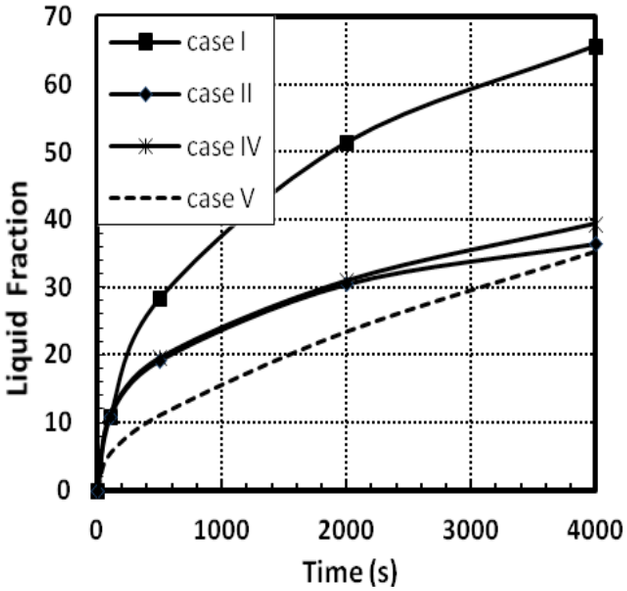

Figure 13. Left: Comparison of liquid fraction between different cases for paraffin wax with 2wt.% of Al_2O_3 Right: Liquid-solid interface at t = 4000 (s) for all cases for paraffin wax with 2wt.% of Al_2O_3.

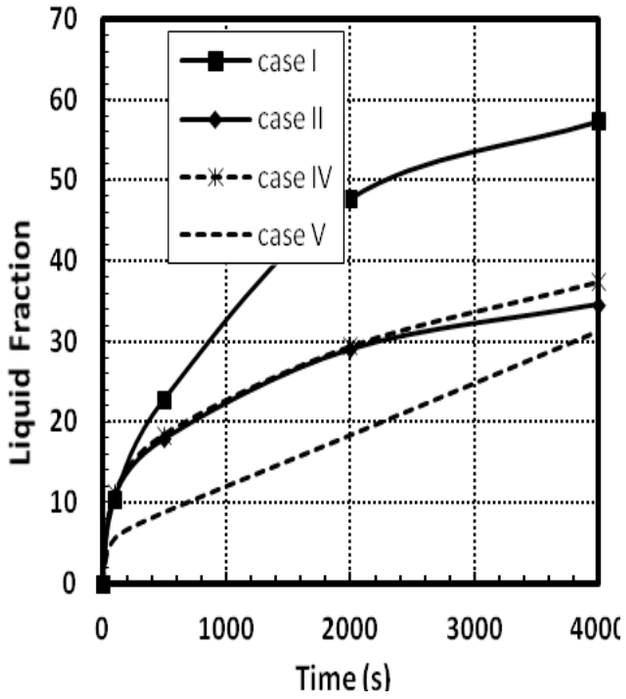

Figure 15. Left: Comparison of liquid fraction between different cases for paraffin wax with 5wt.% of Al_2O_3 Right: Liquid-solid interface at t = 4000 (s) for all cases for paraffin wax with 5wt.% of Al_2O_3.

6. Conclusion

In the present work, melting of a NePCM in a square cavity with different horizontal Source-Sink Positions on the vertical sidewalls is investigated numerically. The governing equations were solved on a non-uniform mesh using a pressure-based finite volume method with an enthalpy porosity technique to trace the solid-liquid interface. Four different cases are studied: in all Cases the source and sink are separately placed on two vertical sidewalls. It was found that, the Case 1 has the highest liquid fraction and the Case 4 possesses the lowest liquid fraction at the final stages of the melting process. In addition, the impacts of the nanoparticle loading are analyzed. In all the cases studied, the volumetric concentration of nanoparticles of 2% would result in the highest melting rate.

7. References

1. Meng E, Yu H, Zhan G, He Y. Experimental and numerical study of the thermal performance of a new type of phase change material room. Energ Convers Manag. 2013; 74(4):386–94.
2. Zhang Y, Chen Z, Wang Q, Wu Q. Melting in an enclosure with discrete heating at a constant rate. Experimental Fluid and Thermal Science. 1993; 6(2):196–201.
3. Faraji M, El Qarnia H. Numerical study of melting in an enclosure with discrete protruding heat sources. Applied Mathematics Modeling. 2010; 34(1):1258–75.
4. Kousksou T, Mahdaoui M, Ahmed A, Msaad AA. Melting over a wavy surface in a rectangular cavity heated from below. Energy. 2014; 64(3):212–9.
5. Available from: http://www.fluent.com
6. Kandasamy R, Wang XQ, Mujumdar AS. Transient cooling of electronics using phase change material (PCM)-based heat sinks. Appl Therm Eng. 2008; 28(5):1047–57.
7. Sasmito AP, Kurnia JC, Mujumdar AS. Numerical evaluation of laminar heat transfer enhancement in nanofluid flow in coiled square tubes. Nanoscale Research Letters. 2011; 6(1):1–14.
8. Arasu AV, Sasmito AP, Mujumdar AS. Numerical performance study of paraffin wax dispersed with Alumina in a concentric pipe latent heat storage system. Thermal Science. 2013; 17(2):419–30.
9. Vajjha RS, Das DK, Namburu PK. Numerical study of fluid dynamic and heat transfer performance of Al2O3 and CuO nanofluids in the flat tubes of a radiator. International Journal of Heat Fluid Flow. 2010; 31(6):613–21.
10. El Hasadi YMF, Khodadadi JM. Numerical simulation of the effect of the size of suspensions on the solidification process of nanoparticle-enhanced phase change materials. J Heat Tran. 2013; 135(5):198–207.
11. Wu SY, Wang H, Xiao S, Zhu DS. An investigation of melting/freezing characteristics of nanoparticle-enhanced phase change materials. Journal of Thermal Analysis and Calorimetry. 2011; 110(2):1127–31.
12. Kashani S, Ranjbar AA, Abdollahzadeh M, Sebti S. Solidification of nano-enhanced phase change material (NEPCM) in a wavy cavity. Heat Mass Tran. 2012; 48(1):1155–66.
13. Hosseinizadeh SF, RabienatajDarzi AA, Tan FL, Numerical investigations of unconstrained melting of nano-enhanced phase change material (NEPCM) inside a spherical container. Int J Therm Sci. 2012; 41(3):77–83.
14. Arasu AV, Mujumdar AS, Numerical study on melting of paraffin wax with Al2O3 in a square enclosure. Int Comm Heat Mass Tran. 2012; 39(6):8–16.
15. Sebti SS, Mastiani M, Mirzaei H, Dadvand A, Kashani S, Hosseini SA. Numerical study of the melting of nano-enhanced phase change material in a square cavity. Journal of Zhejiang University Science A. 2013; 14(5):307–16.
16. Ho CJ, Gao JY. An experimental study on melting heat transfer of paraffin dispersed with Al_2O_3 nanoparticles in a vertical enclosure. Int J Heat Mass Tran. 2013; 62(4):2–8.
17. Zeng Y, Fan LW, Xiao YQ, Yu ZT, Cen KF. An experimental investigation of melting of nanoparticle-enhanced phase change materials (NePCMs) in a bottom-heated vertical cylindrical cavity. Int J Heat Mass Tran. 2013; 66(1):111–7.
18. Khodadadi JM, Hosseinizadeh SF. Nanoparticle-enhanced phase change materials (NEPCM) with great potential for improved thermal energy storage. Int Comm Heat Mass Tran. 2007; 34(5):534–43.
19. Dhaidan NS, Khodadadi JM, Al-Hattab TA, Al-Mashat SM. Experimental and numerical investigation of melting of phase change material/nanoparticle suspensions in a square container subjected to a constant heat flux. Int J Heat Mass Tran. 2013; 66(4):672–83.
20. Dhaidan NS, Khodadadi JM, Al-Hattab TA, Al-Mashat SM. Experimental and numerical study of constrained melting of n-octadecane with CuO nanoparticle dispersions in a horizontal cylindrical capsule subjected to a constant heat flux. Int J Heat Mass Tran. 2013; 67(3):523–34.
21. Dhaidan NS, Khodadadi JM, Al-Hattab TA, Al-Mashat SM. Experimental and numerical investigation of melting of NePCM inside an annular container under a constant heat flux including the effect of eccentricity. Int J Heat Mass Tran. 2013; 67(3):455–68.
22. Jourabian M, Farhadi M, Sedighi K. On the expedited melting of Phase Change Material (PCM) through dispersion of nanoparticles in the thermal storage unit. Comput Math Appl. 2014; 67(6):1358–72.